



Article

Safe Procedure for Efficient Hydrodynamic Gene Transfer to Isolated Porcine Liver in Transplantation

Luis Sendra ^{1,2} Mireia Navasquillo ³, Eva M. Montalvá ^{3,4,5}, David Calatayud ^{3,4}, Judith Pérez-Rojas ⁶ , Javier Maupoey ^{3,4}, Paula Carmona ⁷, Iratxe Zaragoikoetxea ⁷ , Marta López-Cantero ⁷, María José Herrero ^{1,2} , Salvador F. Aliño ^{1,2,*} and Rafael López-Andújar ^{3,4,5}

¹ Pharmacogenetics and Gene Therapy Unit, La Fe Health Research Institute, 46026 Valencia, Spain; luis.sendra@uv.es (L.S.); maria.jose.herrero@uv.es (M.J.H.)

² Gene Therapy and Pharmacogenomics, Department of Pharmacology, University of Valencia, 46010 Valencia, Spain

³ Department of HPB Surgery and Transplantation Unit, Division of General Surgery, University and Polytechnic La Fe Hospital, 46026 Valencia, Spain

⁴ Hepatology, HBP Surgery and Transplants Group, La Fe Health Research Institute, 46026 Valencia, Spain

⁵ Network Biomedical Research Center for Liver and Digestive Diseases, CIBERehd, Health Institute Carlos III, 28029 Madrid, Spain

⁶ Pathology Department, University and Polytechnic La Fe Hospital, 46026 Valencia, Spain

⁷ Anesthesia and Resuscitation Service, University and Polytechnic La Fe Hospital, 46026 Valencia, Spain

* Correspondence: alino@uv.es; Tel.: +34-963-864-972



Citation: Sendra, L.; Navasquillo, M.; Montalvá, E.M.; Calatayud, D.; Pérez-Rojas, J.; Maupoey, J.; Carmona, P.; Zaragoikoetxea, I.; López-Cantero, M.; Herrero, M.J.; et al. Safe Procedure for Efficient Hydrodynamic Gene Transfer to Isolated Porcine Liver in Transplantation. *Int. J. Mol. Sci.* **2024**, *25*, 1491. <https://doi.org/10.3390/ijms25031491>

Academic Editor: Joan Roselló-Catafau

Received: 18 December 2023

Revised: 13 January 2024

Accepted: 18 January 2024

Published: 25 January 2024



Copyright: © 2024 by the authors. Licensee MDPI, Basel, Switzerland. This article is an open access article distributed under the terms and conditions of the Creative Commons Attribution (CC BY) license (<https://creativecommons.org/licenses/by/4.0/>).

1. Introduction

The hydrodynamic procedure for gene transfer consists of the rapid administration of a large volume of saline aqueous solution containing the gene of interest at defined concentrations. This strategy presents the advantage that DNA is administered without any carrier, and then neither toxicity, which is more common with viral vectors [1], nor interactions can occur, and the gene release in the target is not limited [2]. As disadvantages, the gene is delivered without targeting, so it could potentially access any cell, and the volume required for efficient gene transfer could compromise the patient's hemodynamics. The strategy developed in previous works [3] and the present one for loco-regional administration of gene solution in vascular isolated organs permitted circumvention, partially

at least, of these disadvantages since the DNA was injected only in the target organ and the conditions for administration could be moderated. Furthermore, the technique would permit the administration of the gene using minimally invasive catheterization, making its clinical translation feasible [4].

Hydrodynamic injection of naked DNA has been proven to be a safe and efficacious procedure for gene transfer in different organs, especially in the liver. In the early 1990s, it was reported for the first time that DNA could be transferred into the mouse liver by means of its direct injection [5,6]. In 1999, Liu et al. [7] and Zhang et al. [8] described hydrodynamic gene transfer consisting of the rapid injection of a large saline solution volume containing the DNA of interest through the tail vein in mice. Several groups and ours participated in the development of this technique to improve the efficacy of gene transfer and expression. The work of our group, Aliño et al. [9], reported for the first time sustained therapeutic levels of human alpha-1-antitrypsin protein (>1 mg/mL) for periods longer than 6 months after injecting a plasmid containing this entire gene in a murine model of hydrodynamic gene transfer in 2003. Since these promising results, great effort has been made in order to translate this technique to a clinical setting. In this process, different larger animal models have been employed and the conditions of gene injection have been adapted to permit exerting the pressure mediated by the hydrodynamic procedure without affecting the hemodynamic status of the entire body. In this sense, different researchers have proposed distinct pig models [10–13]. The reported results agreed with the suggestion of needing to pressurize the target organ by isolating it from the bloodstream. Our group participated in the translational process employing different porcine models, aiming to exclude the liver vasculature completely or partially, and evaluated the efficiency of gene transfer and decoding. In this regard, we described three models for hydrodynamic gene transfer in the pig liver: open non-invasive catheterization (only one balloon catheter for gene administration in a single lobe with closed backflow) [14]; closed catheterization (three balloon catheters for targeting the whole liver and excluding the entire venous circulation) [15]; and surgery-closed (complete laparotomy for identifying both arterial and venous vessels and targeting the whole watertight liver) [16,17]. We observed that the more the liver was pressurized, the higher the efficacy of expression of the protein encoded by the transferred gene. However, the liver pressurization forced the employment of more invasive procedures.

The porcine model permitted evaluating the potential of this strategy to efficiently transfer a naked entire gene to the liver with enough bioavailability to be decoded and express high levels of the protein of interest. Recently, Kamimura et al. [18] reported efficient gene transfer in the baboon liver by lobe-directed hydrodynamic injection employing IX coagulation factor. Aiming to determine whether this would occur in human beings, we developed a procedure to transfer a gene using the hydrodynamic procedure in watertight human liver segments derived from surgical resection in patients with cancer [19]. After gene transfer, tissue samples were cultured and the process of gene decoding was quantified at different time points. This study proved that, despite the fact that the liver had been removed from a patient and had no nutrients and oxygen supply, human liver tissue could efficaciously express the gene for some days.

The procedure demonstrated its potential to efficiently transfer genes to the porcine and human liver; however, the need for organ pressurization and the large volumes injected (≥ 200 mL) in a short time (approx. 20 s) made its clinical application unacceptable. For this reason, we decided to test it in a clinical setting that could benefit from this procedure without affecting the patient. In this respect, liver transplantation offers an opportunity for safe gene transfer in a watertight organ during the bench surgery step between organ collection and its implantation in the recipient. In this stage, surgeons have access to the entire vasculature [20]. Hence, the liver could be safely pressurized and the gene hydrodynamically transferred to the entire organ without affecting either the regular performance of organ transplantation or the hemodynamic status of the patient.

One of the main limitations of liver transplantation is immunosuppression. Despite the substantial efficacy of calcineurin inhibitors, post-transplantation early mortality remains as high as 5–12%, and acute cellular rejection appears within the first year post-intervention in 25–30% of patients [21] or more [22]. For this reason, it was decided to employ a gene that encoded a protein with immunomodulatory function, interleukin-10, instead of a tracer gene, GFP, since this cytokine plays a central role in the modulation of immune activation through different pleiotropic functions. Interleukin-10 (IL-10) is a pleiotropic cytokine that plays a fundamental role in modulating inflammation and maintaining cell homeostasis. It primarily acts as an anti-inflammatory cytokine, protecting the body from an uncontrolled immune response. Given the pivotal role of IL-10 in immune modulation, this cytokine could have relevant implications in pathologies characterized by the hyperinflammatory state. IL-10 leads to the shutdown of the inflammatory immune response, both directly, by the suppression of macrophage and dendritic cell activity, and indirectly, by limiting T cell activation, differentiation, and effector function, and promoting peripheral tolerance [23].

This molecule was reported to improve the outcome in transplantation [24] and polymorphisms in its gene have been described to influence transplantation success. Additionally, we selected it because it could also serve as tracer molecule at the RNA and protein levels to permit differential quantification of the expression of the exogenous human gene. It has been reported that the amino acid sequence homology between human and mouse, rabbit, pig, and cow IL-10 is high. Human and porcine IL-10 proteins present 76% homology, more than that observed between human and mouse proteins. Human IL-10 cDNA presents important homology with pig IL-10, with 82% homology in the nucleotide sequence [25]. Moreover, IL-10 has been shown to be functionally active across species barriers, including human, mouse, rabbit, pig, and cow [26–28].

In the present work, an orthotopic liver transplantation porcine model with standard immunosuppressant treatment was employed to hydrodynamically transfer the human IL-10 gene to the graft liver during bench surgery, as previously described [14–17,19]. Our main goal was to evaluate the aspects related to the pharmacokinetics of the procedure of gene delivery to mediate protein expression in the blood and the further potential effect of IL-10 in the immediate post-transplantation expression of cytokines for 10 days.

Collectively, the procedure proved to be safe and permitted the efficient expression and plasma release of human IL-10 protein, achieving sustained levels during the entire follow-up with potential immunosuppressive activity without any damage with respect to control group animals.

2. Results

2.1. Biochemical Variables and Liver Function

Although differences were observed between the control and treated groups at some time points, none of the determined parameters (Table 1; Figure 1) showed statistically significant differences between groups. In spite of these differences, the observed levels did not exceed safety values in any case and tended to normalize after 1 day post-surgery.

Table 1. Biochemical parameters in plasma after liver transplant. N: 5 pigs per group. Dose: 20 µg/mL; 200 mL; 20 mL/s.

	pH		Creatinine (mg/dL)				Lactate (mmol/L)				Hemoglobin (g/dL)						
	Control		IL-10-Treated		Control		IL-10-Treated		Control		IL-10-Treated		Control		IL-10-Treated		
	Average	SD	Average	SD	Average	SD	Average	SD	Average	SD	Average	SD	Average	SD	Average	SD	
Pre-surgery	7.39	0.04	7.06	0.50	1.20	0.14	ND	ND	1.18	0.32	0.57	0.00	8.85	1.91	ND	0.00	
	7.49	0.05	7.44	0.07	1.70	0.10	1.33	0.15	1.15	0.53	1.44	0.21	8.60	1.39	9.14	0.93	
	7.52	0.03	7.48	0.01	1.25	0.07	1.15	0.17	0.79	0.17	0.72	0.18	7.80	0.00	8.30	1.04	
	7.47	0.05	7.48	0.01	1.13	0.10	1.17	0.06	0.77	0.19	1.13	0.32	8.30	0.81	9.88	1.96	
	7.49	0.03	7.48	0.04	1.15	0.31	1.05	0.06	1.01	0.48	1.17	0.34	7.93	1.12	10.40	2.08	
	7.42	0.10	7.41	0.08	1.07	0.21	0.97	0.15	1.84	1.44	1.27	0.73	8.27	0.50	9.63	1.40	
Bilirubin (mg/dL)																	
		Control		IL-10-Treated		Control		IL-10-Treated		Control		IL-10-Treated		Control		IL-10-Treated	
		Average	SD	Average	SD	Average	SD	Average	SD	Average	SD	Average	SD	Average	SD	Albumin (g/L)	
1 d	0.46	0.18	0.33	0.13	88.25	9.50	104.60	31.39	25.50	5.80	25.80	—	—	—	—	2.86	
	0.35	0.24	0.47	0.18	101.00	37.42	88.40	11.63	24.20	1.92	28.20	—	—	—	—	2.28	
	0.50	0.33	0.64	0.36	87.00	10.93	63.60	34.34	24.60	2.51	26.20	—	—	—	—	2.05	
	0.54	0.28	0.84	0.64	83.60	9.34	52.00	37.40	23.80	3.56	25.20	—	—	—	—	2.77	
	0.78	0.55	0.91	0.65	78.67	17.16	69.50	20.86	25.67	2.52	28.75	—	—	—	—	5.25	

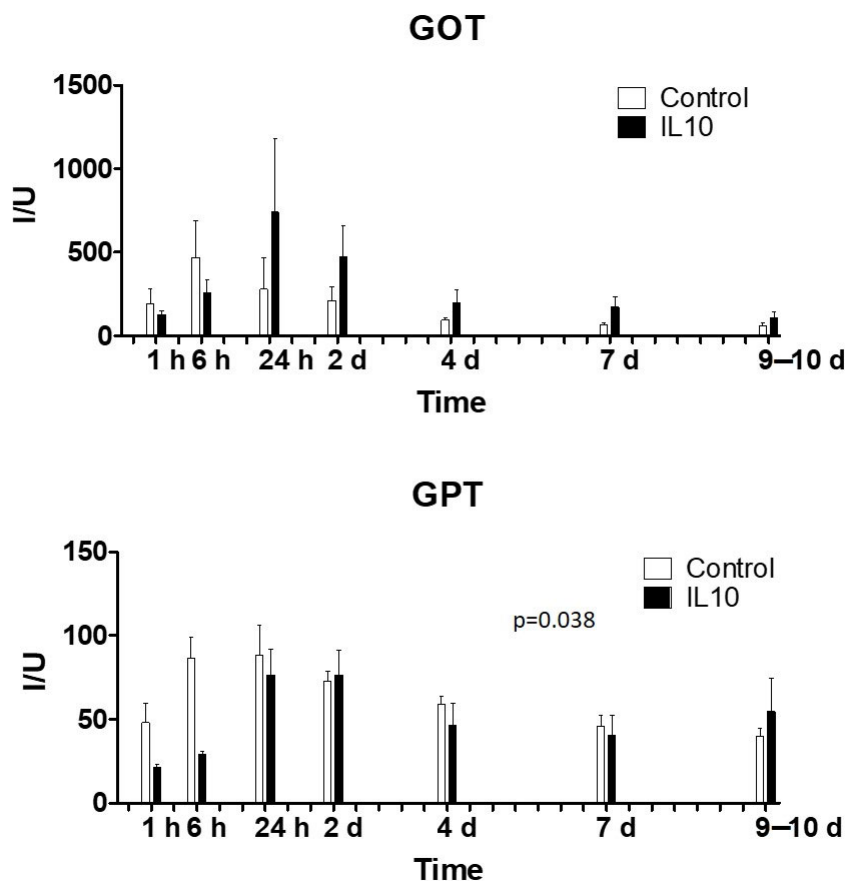


Figure 1. Liver enzymes in plasma after liver transplant. GOT: Glutamate-oxaloacetate transaminase or aspartate aminotransferase; GPT: Glutamic-pyruvic transaminase or alanine aminotransferase. p -value GOT = 0.35; p -value GPT = 0.24. N: 5 pigs per group. Dose: 20 μ g/mL; 200 mL; 20 mL/s.

2.2. Human IL-10 Protein Concentration in Plasma

Human IL-10 protein (Figure 2) in treated animals achieved stable plasma concentrations over 20 pg/mL until day 10, with a near 40 pg/mL peak on day 2, which was higher ($p = 0.012$; t -test) than in control animals, in which concentrations remained around the detection threshold during the entire follow-up.

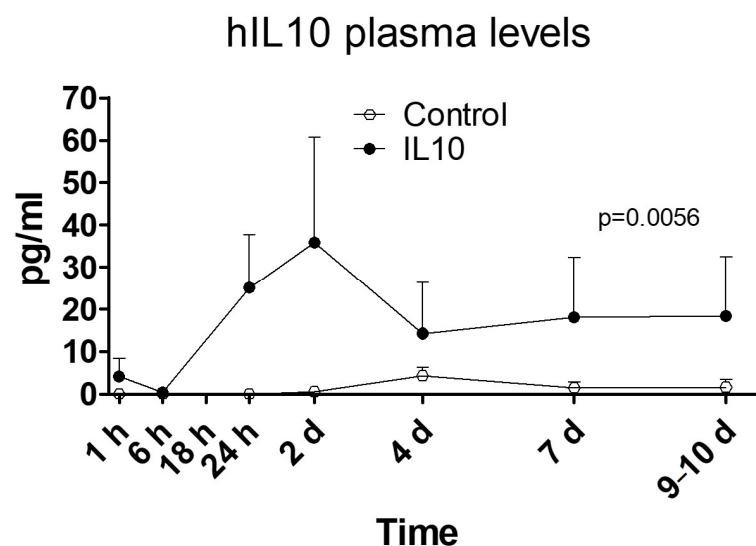


Figure 2. hIL-10 protein in plasma. Protein was quantified by ELISA in plasma from blood samples obtained during the follow-up. N: 5 pigs per group. Dose: 20 μ g/mL; 200 mL; 20 mL/s.

2.3. Human IL-10 RNA Expression in Liver Tissue Samples

Figure 3 shows the tissue amount of human IL-10 RNA in the different areas of the liver, expressed as copy number per cell after subtracting the background read. All liver lobes presented detectable expression of *hIL-10* mRNA, although the yield was different depending on the area of the organ. Whereas both medial and lateral segments of the right lobes showed similar intermediate transcription rates, in the left lobes, great differences between the medial and lateral areas were detected, the latter showing the lowest efficacy. The proximal area of the medial left lobe showed the highest production of mRNA, more than 1000-fold higher than in the lateral left segments. We think that the reason for such differences must be the anatomical structure of the suprahepatic vasculature that orientates the catheter in that direction and favors the irrigation of those areas.

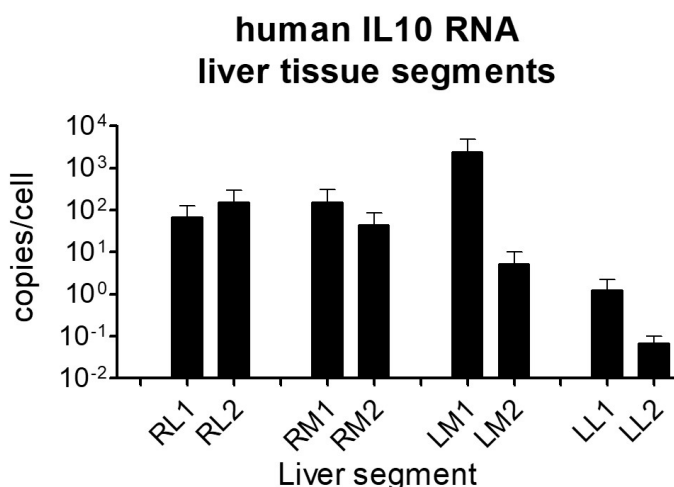


Figure 3. *hIL-10* RNA tissue expression. Tissue samples from 8 different liver areas were collected and the RNA was extracted and retrotranscribed. *hIL-10* cDNA was quantified by qPCR and expressed as copies per cell. The unspecific values obtained in control animal samples were considered as the threshold and subtracted from the levels obtained in samples from transfected animals. RL: right lateral; RM: right medial; LM: left medial; LL: left lateral; 1: proximal; 2: distal. N: 5 pigs per group. Dose: 20 µg/mL; 200 mL; 20 mL/s.

2.4. Expression of Porcine Interleukin-10

The *hIL-10* liver gene transfection did not alter the expression of natural porcine IL-10 and, thus, no difference between the treated and control groups ($p = 0.393$) was observed (Figure 4).

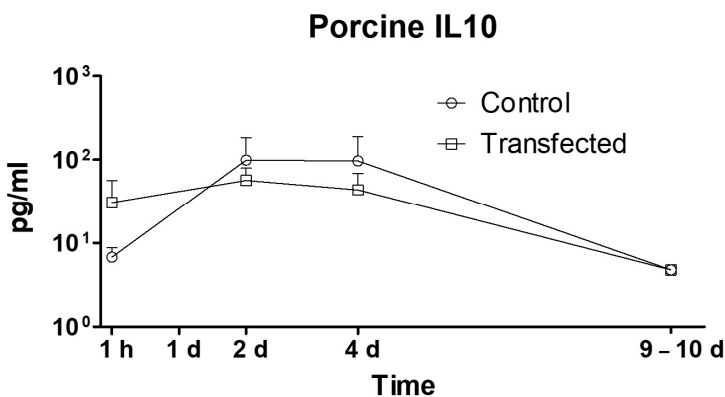


Figure 4. Porcine IL-10 protein in plasma. Protein was quantified in plasma from blood samples obtained during the follow-up using a Magpix Multiplex analyzer, based on fluorescence microscopy and flow cytometry. Levels achieved in control and treated animals were not significantly different ($p = 0.39$; t-test). N: 5 pigs per group. Dose: 20 µg/mL; 200 mL; 20 mL/s.

2.5. Plasma Levels of Other Porcine Cytokines

Several cytokines involved in the immune response were quantified in blood samples. Except for interferon gamma and pIL-10, levels of all determined cytokines were higher in the DNA-transfected group. Levels of tumor necrosis factor- α (TNF- α), interleukin-1 β (IL-1 β), interleukin-4 (IL-4), interleukin-6 (IL-6), and interleukin-8 (IL-8) were higher from the beginning of sample collection (1h) in transfected animals and their levels were sustained during the entire follow-up (Figure 5A), with significantly different behavior ($p = 0.0017$, $p = 0.0141$, $p = 0.0054$, $p = 0.0046$, and $p = 0.0057$, respectively). Interferon- α (IFN- α) and interferon- γ (IFN- γ) presented similar expression profiles in both groups (Figure 5B). Although it was not significant ($p = 0.089$), the expression of IFN- α increased in the transfected group during the first 2 days, maybe due to the administration of double-stranded DNA, as previously reported. Nucleic acids derived from pathogens or released from damaged cells can activate the immune system. TLR9, a membrane-bound DNA sensor, detects CpG DNA at the endosome to induce type I IFN production. There are also TLR9-independent pathways that can recognize double-stranded DNA (dsDNA) in the cytoplasm, preferentially mediating the production of IFN- α but not IL-12 [29,30]. Interleukin-12 (IL-12) expression levels in transfected pigs were significantly higher ($p = 0.0001$) during the follow-up, and this could be due to an immune response against the presence of ssRNA in the bloodstream, which could happen since the administered plasmid had already been proven to express *hIL-10* mRNA in few hours [17,19]. RNA-sensing mechanisms are mediated by Toll-like receptors (TLR) and by retinoic acid-inducible gene I-like receptors (RLRs), which induce the secretion of IL-12 but not IFN- α [29,30]. Plasma levels of immunomodulatory cytokine TGF- β (transforming growth factor- β) were significantly higher ($p = 0.0323$) in transfected animals during the entire follow-up.

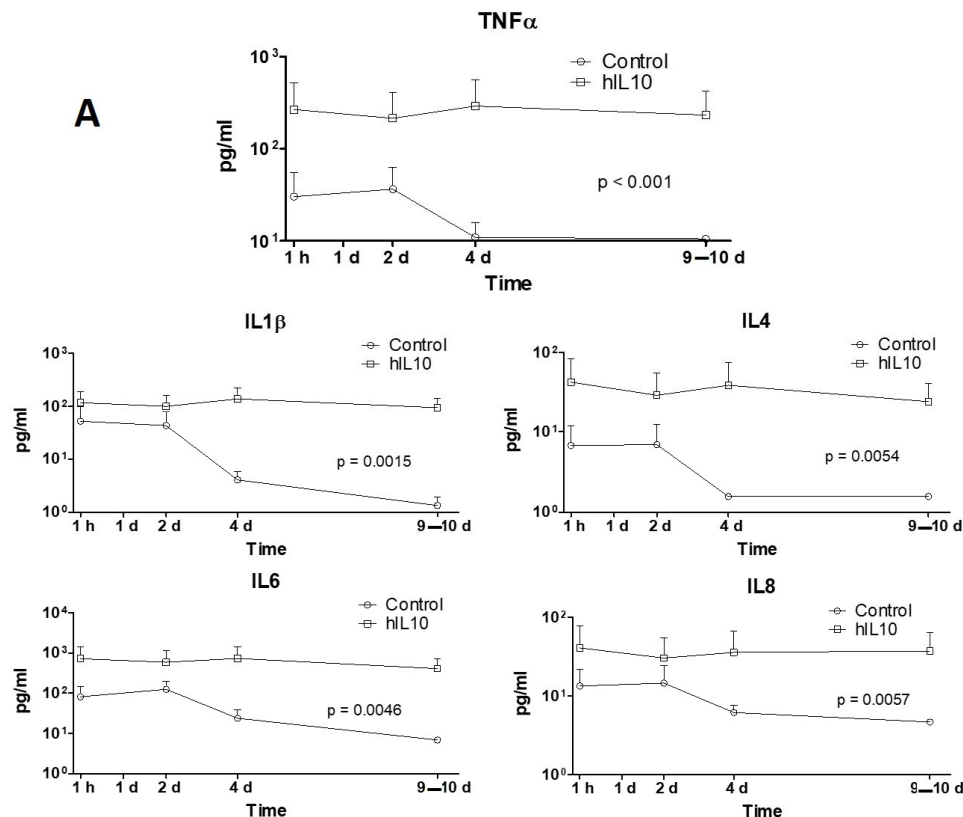


Figure 5. Cont.

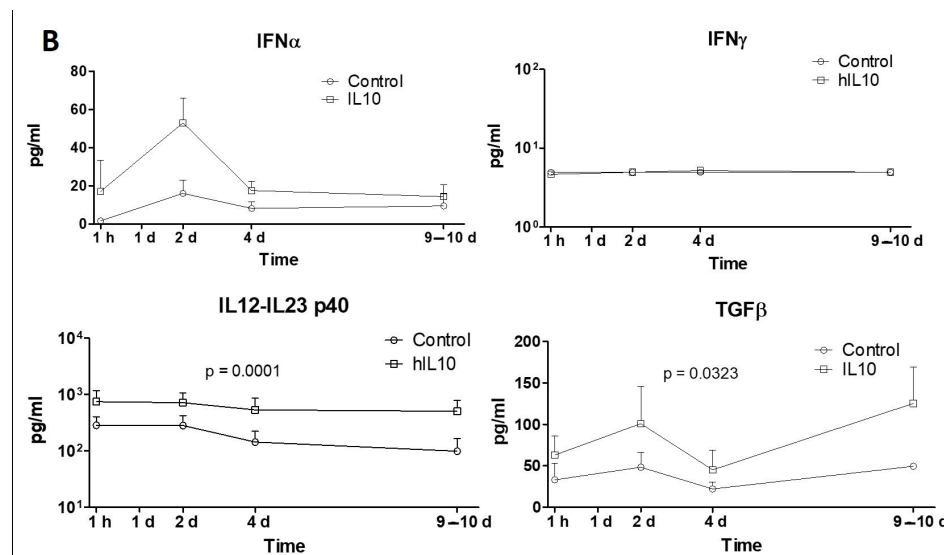


Figure 5. (A) Plasma levels of porcine cytokines TNF α , IL1 β , IL4, IL6 and IL8. (B) The levels of IFN α , IFN γ , IL12-IL23 p40 and TGF β . Proteins were quantified in plasma from blood samples obtained at different time points during the follow-up using a Magpix Multiplex analyzer, based on fluorescence microscopy and flow cytometry. Statistical test: t -test. N: 5 pigs per group. Dose: 20 μ g/mL; 200 mL; 20 mL/s.

2.6. Histological Evaluation of Liver Injury

In spite of immunosuppressant treatment, we observed three cases of acute rejection, two in the treated group (one of them very incipient and light) and another one in the control group. To precisely define the liver acute rejection, we classified the different types and level of liver injury observed in the histologic preparations. In Figure 6A, representative images of the general injury signs observed, such as ischemic injury and unspecific inflammation, are shown. In Figure 6B, acute rejection signs based on Banff parameters, such as duct injury, portal inflammation, and venular inflammation, can be observed.

To differentiate the potential effects of IL-10 modulatory gene injection, a pathologist assigned quantitative severity values (0–3) to the injury effects observed in the samples of each animal. No statistical difference in general damage was observed between the control and treated groups. Although rejection appeared in one only animal per group, the severity of the overall score of acute rejection signs (Figure 7) was higher in the control pig (7.5 vs. 4.25, $p = 0.043$).

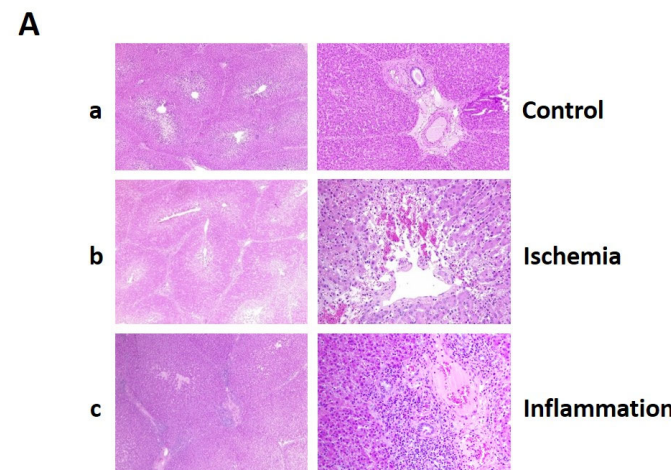


Figure 6. Cont.

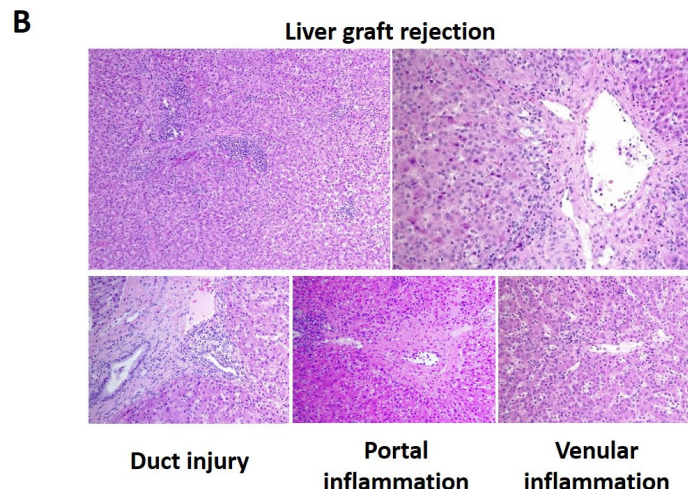


Figure 6. Images of general injury (A) and signs of acute rejection (B) in liver tissue samples under a bright microscope at 10 \times and 20 \times magnification after hematoxylin-eosin staining. In panel A, left pictures were taken at 10 \times magnification and right pictures at 20 \times . (A) a images represent healthy control tissue without damage; b pictures show a tissue sample with ischemia and c image shows an area of liver sample with inflammation and cell infiltration. Superior left picture in panel (B) shows a general view of tissue sample (10 \times) from a liver with rejection signs. Other images are details (20 \times) of the sample showing typical Banff rejection signs.

Liver injury after transplantation

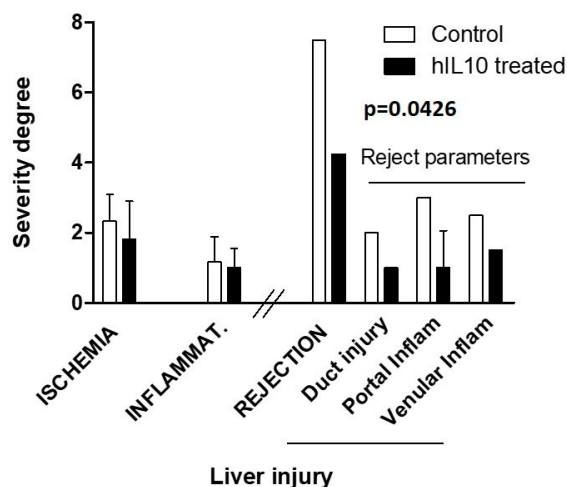


Figure 7. Graph representing the general injury and acute rejection degree of severity in liver tissue samples assigned by a blinded pathologist. Each of these signs received a value from 0 to 3 depending on their severity in each individual sample. These were aggregated and averaged for each animal to establish its overall damage. Statistical test: t -test. N : 1 pig per group presenting rejection signs). Dose: 20 μ g/mL; 200 mL; 20 mL/s.

3. Discussion

The aim of this study was to evaluate the efficiency of the hydrodynamic injection procedure to mediate hepatic *hIL-10* gene transfer with bioavailability for decoding, express the protein in the bloodstream in a model of liver transplantation, and evaluate the acute effect on cytokine release in the immediate post-transplantation stage. Following gene transfection, transcription of *hIL-10* RNA was distributed throughout all liver lobes (0.1 to 1000 copies per cell, depending on the area) and sustained levels of human IL-10 protein over basal functional levels were observed (20 pg/mL) during the follow-up period,

indicating successful gene transfer. Interestingly, we observed overall increments in both anti- and pro-inflammatory cytokines, which did not correlate with more severe liver injury.

The *hIL-10* gene was selected since it could serve as a tracer due to the ability to differentiate porcine and human proteins, interest in its use in liver transplantation, and our previous knowledge of its physiology and expression profile. The plasmid was injected under optimal conditions, previously established by our research group, into a watertight liver on the surgical bench immediately before implantation. No statistical differences were found in plasma levels of biochemical parameters, except for albumin and liver enzymes, suggesting that the gene transfer did not affect normal liver function.

In the treated animals, *hIL-10* concentrations reached a peak of 40 pg/mL on day 2, followed by a decrease to 20 pg/mL, which remained stable until day 10. This indicated that the plasmid successfully reached the cells, underwent transcription to RNA, translation to protein, and release into the bloodstream. These levels were expected to mediate an immunomodulatory effect, considering that the calculated half-maximal inhibitory concentration (IC₅₀) of IL-10 for TNF- α is 124 pg/mL [31]. The local concentration achieved in the liver environment was likely higher, highlighting the potential clinical relevance of this procedure. Notably, the porcine IL-10 plasma levels (100 pg/mL) in both groups were higher than those of the human protein (20–40 pg/mL). We assume that the effect must have been induced by the increase in human protein concentration, since although we cannot rule out the possibility of a synergistic effect between human and porcine interleukin-10 on the expression of other cytokines, we only observed differences in human IL-10 expression between the control and treated groups.

Despite the increased and sustained expression of both pro- and anti-inflammatory cytokines after *hIL-10* transfection, the *hIL-10*-treated animals generally displayed better wellbeing, as observed through their behavior and response to stimuli. In accordance with the levels of analyzed cytokines, one would anticipate that pigs treated with IL-10 would exhibit a greater and sustained inflammatory response throughout the entire study duration. Mediators conventionally reported as pro-inflammatory and, consequently, of potential risk for transplant evolution [32] (IL-1, IL-6, IL-8, TNF- α , IL-12–IL-23) maintained higher levels throughout the analysis period in the treated pigs compared to the controls, where they normalized by days 2–4 post-intervention. However, assessment of anatomo-pathological parameters indicated that the severity of Banff parameters, used to define the onset of rejection, was significantly higher ($p = 0.0426$) in the case in the control group. Conversely, levels of proteins with potential anti-inflammatory roles (IL-10, TGF- β) were also elevated in the treated pigs, which could favor the establishment of tolerance. These findings would require confirmation in longer-term studies wherein the Treg response could be assessed. These pleiotropic cytokines are known to participate in various activation or modulation [33,34] pathways during the acute phase of inflammation. Aiming to understand this pleiotropic response in the acute phase, we summed up the available information in Figure 8, where the signaling of interleukins, antigen activation, and effects of the immunosuppressant drug, tacrolimus, are represented as responsible pathways for the final activating or suppressant response.

In our study, immune activation mediated by MHC antigen recognition initiates the expression of IL-2 and clonal cell expansion. This cytokine activates its own receptor, promoting T cell proliferation, also including the generation of immunosuppressive Treg cells through the expression of Foxp3 [35]. However, calcineurin inhibitors block the production of IL-2, limiting the establishment of late immune tolerance mediated by Tregs [36]. Interleukin-10 (IL-10) is a pleomorphic cytokine produced by most activated immune cells, including B cells, mast cells, granulocytes, macrophages, dendritic cells, and multiple T cell subsets such as Tregs. Receptor ligation activates JAK/STAT3 signaling, leading to changes in the expression of immunomodulatory genes, such as Foxp3, inhibiting pro-inflammatory mediators, decreasing antigen presentation, and enhancing the tolerance functions of these cells. IL-10 can act as a feedback regulator that affects the control and resolution of inflammation via autocrine and paracrine mechanisms. In addition, IL-10 is

thought to inhibit apoptotic signaling pathways, such as the p38 MAPK (mitogen-activated protein kinase) pathway, and maintain and expand Treg cell populations [37]. On the other hand, IL-10 can positively enhance activation and proliferation of certain immune cell types, including mast cells, CD8+ T cells, NK cells, and B cells, although the molecular mechanisms and functional consequences of such activity remain to be elucidated [38].

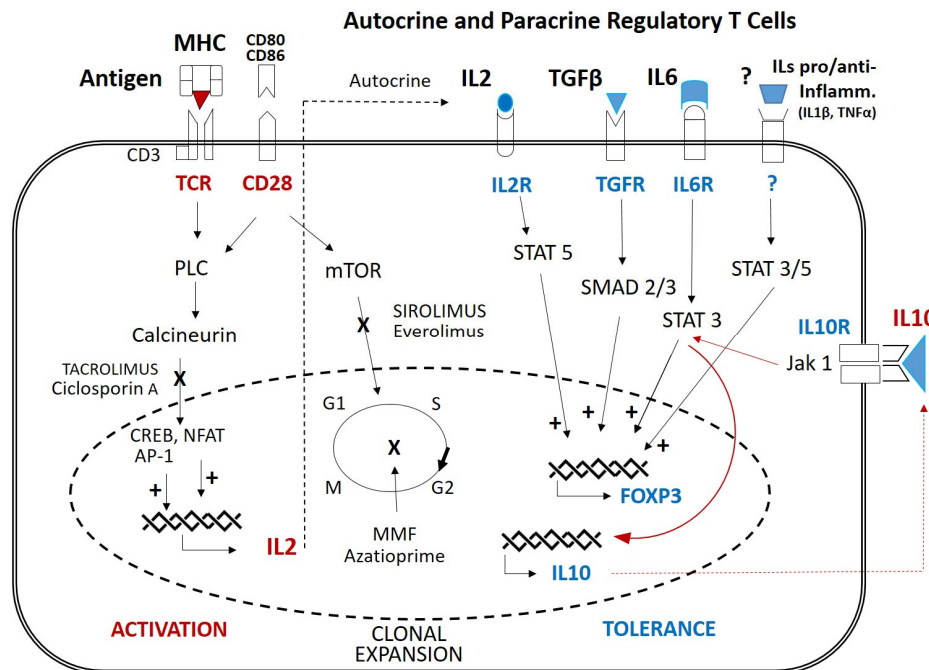


Figure 8. T cell activation/tolerance and mechanisms involved. MHC: major histocompatibility complex; TCR: T cell receptor; CD: cluster of differentiation; MMF: mycophenolate mofetil; PLC: phospholipase C; NFAT: nuclear factor of activated T cells; CREB: CAMP response element-binding protein; AP-1: activator protein 1; STAT: signal transducer and activator of transcription; SMAD: suppressor of mothers against decapentaplegic; mTOR: mammalian target of rapamycin; Jak: Janus kinase.

In this regard, we observed that IL-10 gene transfection increased the expression of IL-6 (STAT3) and TGF- β (SMAD2/3) [39], which we conjecture may compensate for the decrease in Foxp3 expression through different pathways than those employed by IL-2 (STAT3/5) [40]. Additionally, interleukin-10 could directly mediate the maintenance of Tregs [41] and indirectly induce the expression of TGF- β [39,42], although this should be confirmed in further longer-term dose-response studies. The direct action of IL-10 on Tregs through the Jak1/STAT3 signaling pathway could be responsible for enhancing the autocrine production of IL-10, and this could control the feedback response and possibly the expansion of Treg cells [43].

4. Materials and Methods

4.1. Animals

All animals received human care according to the “Guide for the Care and Use of Laboratory Animals”. Female 3-month-old pigs (25–30 kg) were individually housed in pigsties. Anesthesia was induced with ketamine (5–10 mg/kg, IM), midazolam, (0.3 mg/kg, IM), and propofol (4–6 mg/kg, IV). For its maintenance, inhaled sevoflurane was used (2%). All pigs were intubated for mechanical ventilation. Intra-intervention analgesia was achieved with fentanyl (10 μ g/kg, IV, each 30 min) and buprenorphine (0.02 mg/kg, IV). The latter was also employed for post-surgery control of pain (0.15 mg/12 h until day 4, then it was reduced by half or removed). If fever appeared, intravenous meloxicam was scheduled. In the recipients, a central 3-way catheter was placed in the jugular vein for drug administration and blood samples collection, and an intra-arterial one was inserted in

the femoral artery for pressure monitoring and intraoperative blood sampling. Antibiotic (amoxicillin/clavulanic acid, 250 mg, IV) was administered during the intervention and each day during the stabilizing period. All pigs, control (*n*: 5) and treated (*n*: 5), received immunosuppressant treatment as usual. These drugs were tacrolimus (0.04 mg/kg, per day, IV; this could be switched to oral Advagraf® (Astellas pharma Europe, Addlestone, UK) if parenteral intolerance appeared) and methylprednisolone in a 6-day tapering dosage regimen (500 mg intra-intervention, 125 mg, 100 mg, 75 mg, 50 mg, and 25 mg, per day, IV). Electrocardiogram, oxygen saturation, arterial and venous pressures, and PETCO₂ were also monitored during the procedure. Blood gas determinations were performed during dissection and the anhepatic and reperfusion stages to evaluate the condition of the animal and adjust the administration of drugs and fluids. From day 1 onwards, omeprazole was administered (20 mg/day, IV) to avoid potential drug-derived gastric damage. The experiments were approved by the Animal Biological Research Ethics Committee of Hospital La Fe (ref. 2018/VSC/PEA/0145; Date of approval 2 July 2018).

4.2. Surgical Procedure

4.2.1. Donor

After anesthesia induction and hemodynamic control, the surgical procedure was carried out as described by Fondevila et al. [44] with few modifications and the follow-up period was doubled. In brief, a midline xiphopubic laparotomy was performed. Then, the liver pedicle elements (bile duct, portal vein, and hepatic artery) were located and dissected as distally as possible. Bile duct was flushed with 100 mL saline solution; intravenous sodium heparin (3 mg/kg) was administered. After 3 min, the portal vein and aorta artery were cannulated and the liver was perfused with cold Celsior® (Institute Georges Lopez, IGG, Lissieu, France) preservation solution, and it was exsanguinated by an excision in the inferior vena cava. After cold perfusion, complete hepatectomy was performed.

4.2.2. Bench Surgery and Gene Transfer

Immediately after the hepatectomy, the organ was prepared on the bench. The inferior vena cava was sectioned at the diaphragm, and all branches of the celiac arterial trunk and the portal vein were preserved for as long as possible. In all livers, cholecystotomy was performed and the cystic duct was resected. Then, the liver was cold-preserved in Celsior® at 4 °C. In the case of control pigs, no further intervention was required until the graft implant. In *hIL-10* plasmid-treated pigs, the gene was hydrodynamically transferred as follows: the inferior vena cava was clamped in both extremes, the portal vein and liver artery were also closed, and the gene (20 µg/mL in 200 mL saline solution) was retrograde-injected through the suprahepatic vein at 20 mL/s. The liver was maintained watertight for 5 min. After this time, the clamps were removed and the organ was ready to be implanted.

4.2.3. Recipient

Classic hepatectomy without inferior vena cava preservation was performed, as previously described. In brief, the liver hilum elements were dissected following this order: bile duct, right and left hepatic arteries, and portal vein. Then, the triangular and gastrohepatic ligaments were sectioned to completely liberate and mobilize the liver. Both the supra- and infrahepatic inferior vena cava were dissected. Then, the cava, portal, and hepatic veins were clamped. The elements of the pedicle, hepatic veins, and cava were sectioned and the liver was removed. This anhepatic stage had to be rapid and it did not last more than 20–25 min since this would compromise the safety of the procedure and the recipients' survival. The graft implant phase started with the anastomosis of the donor's and recipient's suprahepatic inferior vena cava. Then, the portal vein was anastomosed and these vessels were declamped to reduce intestinal ischemia and favor venous return. Subsequently, anastomosis of the infrahepatic vena cava was performed and the clamps were removed, thus improving the hemodynamic status of the pig due to complete venous reperfusion. Then, the hepatic artery was anastomosed, controlling its length in order to be

neither twisted nor redundant. Finally, the bile duct was also anastomosed with the aid of a silicone tube inserted as an internal tutor. Then, the abdominal cavity was cleaned and the abdominal wall was closed.

4.3. Post-Transplantation Care

Pigs were monitored every 8 h from intervention until sacrifice, evaluating their stance, breathing, food intake, and response to stimuli. The medication described above was administered during the stablizing period through the 3-way catheter placed in the jugular vein.

4.4. Plasmid

Plasmid p2F-hIL-10 (6.86 Kb), containing human IL-10 cDNA driven by the pCMV promoter, was constructed by cloning IL-10 into the HindIII site of pVITRO2 (Invitrogen, Thermo Fisher, Waltham, MA, USA).

4.5. Biochemical Parameters and Liver Enzymes Determination

Blood biochemical parameters were quantified ‘in situ’ using the i-STAT 1[®] blood analyzer (Abbott Laboratories, Chicago, IL, USA) during the intervention and the entire period of stablizing from the jugular vein. Two different analysis cartridges were employed: CG4+ (lactate, pH, pCO₂, pO₂, TCO₂, HCO₃, sO₂, base excess or BE); and CG8+ (sodium, potassium, ionized calcium, glucose, hematocrit, hemoglobin). Plasma GOT and GPT were quantified post-intervention by an external laboratory employing an electrochemical method.

4.6. Quantitative PCR and RT-PCR

Tissue samples representing the whole liver were collected after sacrifice and homogenized in buffer (Promega[®], Madison, WI, USA) using an Ultra-Turrax homogenizer (Hielscher Ultrasonics GmbH, Teltow, Germany). Further purifications were performed using the Maxwell RNA Purification From Tissue Kit (Promega[®], Madison, WI, USA) before spectrophotometric quantification. RNA retrotranscription to cDNA was carried out using the High Capacity cDNA Archive Kit (Thermo Fisher[®], Waltham, MA, USA). For real-time qPCR, TaqMan PCR Master Mix (Thermo Fisher[®], Waltham, MA, USA) was employed according to the instructions of the manufacturer. The specific oligonucleotides for the human IL-10 employed were from a pre-mixed kit from Thermo Fisher (cat no. Hs00961622_m; Thermo Fisher[®], Waltham, MA, USA).

4.7. Cytokine Determination

4.7.1. hIL-10 ELISA

Blood samples were collected at 1 h, 6 h, 1 day, 2 days, 4 days, 7 days, and 10 days after gene transfer. Plasma was separated and the protein presence was determined. For human IL-10 quantification, the BD OptEIA[®] Human IL-10 ELISA Set (Becton and Dickinson Biosciences, Franklin Lakes, NJ, USA) was used, following the manufacturer’s instructions.

4.7.2. Determination of Porcine Cytokines

Blood samples were collected at 1 h, 2 days, 4 days, and 10 days post-transplantation. Cytokine concentrations in plasma were quantified using a Magpix Multiplex analyzer (Luminex, Austin, TX, USA), based on fluorescence microscopy and the flow cytometry technique. We simultaneously determined IL-1 β , IL-4, IL-6, IL-8, IL-10, IL-12–23, 40p, IFN- α , IFN- γ , and TNF- α , employing the Cytokine & Chemokine 9-Plex Porcine ProcartaPlexTM (Invitrogen, Waltham, MA, USA), following the manufacturer’s instructions. TGF- β was separately quantified using the TGF beta 1 Porcine ProcartaPlexTM Simplex Kit (Invitrogen, Waltham, MA, USA).

4.8. Anatomopathological Evaluation of Tissue Samples

After the stabiling period, animals were sacrificed and tissue samples ($2\text{ cm} \times 1\text{ cm} \times 2\text{ mm}$) from all liver lobes were collected and preserved in formaldehyde. Tissue slides were stained with hematoxylin-eosin and observed under an optical microscope at $10\times$ and $20\times$ magnification. Different injury signs were evaluated and classified as intervention-derived parameters, such as ischemic lesions and general inflammation traces, and organ rejection, defined by the Banff triad (duct injury, portal inflammation, and venular inflammation). A Liver Transplantation Hospital anatomopathologist assigned a severity value from 0 to 3 to each injury sign in each sample in a blind study. The values were aggregated and averaged for each animal to establish its overall damage, separating intervention-derived injury from rejection.

4.9. Statistical Analyses

Results obtained in the transfected and control groups were compared statistically with a paired *t*-test, employing Prism 5 software (Graphpad Software, Carlsbad, CA, USA), and *p*-value was considered significant from 0.05 downwards. Data graphing was performed using the same software.

5. Conclusions

In conclusion, our study supports that hydrodynamic transfer of the naked human IL-10 gene in the liver transplantation setting is a safe, viable, and efficient procedure for achieving sustained plasma levels of human protein with potential functional activity. This increased protein expression was associated with elevated levels of both pro- and anti-inflammatory cytokines, which did not lead to significant liver tissue injury. Moreover, we observed elevated plasma levels of some cytokines known for their capacity to mediate immunotolerance activity, such as TGF- β and IL-6, which could facilitate the graft tolerance process. In this regard, the pharmacokinetics (production and release to blood-stream of interleukin-10) of the procedure were verified and when translated to humans, the pharmacodynamics (drug-receptor) process would require additional dose-response (hydrodynamic gene transfer efficacy is dose-dependent and the doses employed in this study could be largely augmented) and longer-term studies.

Author Contributions: Conceptualization, S.F.A. and R.L.-A.; methodology, L.S., M.N., E.M.M., I.Z. and D.C.; software, L.S.; validation, S.F.A., R.L.-A. and E.M.M.; formal analysis, M.J.H. and D.C.; investigation, J.M., J.P.-R., M.L.-C. and P.C.; resources, M.N., I.Z. and J.P.-R.; data curation, L.S. and S.F.A.; writing—original draft preparation, L.S. and M.N.; writing—review and editing, S.F.A., R.L.-A. and E.M.M.; visualization, I.Z. and M.J.H.; supervision, E.M.M.; project administration, L.S. and R.L.-A.; funding acquisition, R.L.-A. All authors have read and agreed to the published version of the manuscript.

Funding: This work has been funded by ‘Fundación Mutua Madrileña’, project number 2017/0270.

Institutional Review Board Statement: The animal study protocol was approved by the Institutional Ethics Committee of Hospital La Fe (ref. 2018/VSC/PEA/0145; Date of approval: 2 July 2018).

Informed Consent Statement: Not applicable.

Data Availability Statement: Data are contained within the article.

Acknowledgments: We would like to thank Javier Sicilia for his effort that made this work possible and Inmaculada Noguera and Ana Díaz for their valuable help.

Conflicts of Interest: The authors declare no conflicts of interest.

References

1. Buchwald, J.E.; Martins, P.N. Designer organs: The future of personalized transplantation. *Artif. Organs* **2022**, *46*, 180–190. [[CrossRef](#)] [[PubMed](#)]
2. Huang, M.; Sun, R.; Huang, Q.; Tian, Z. Technical Improvement and Application of Hydrodynamic Gene Delivery in Study of Liver Diseases. *Front. Pharmacol.* **2017**, *8*, 591. [[CrossRef](#)] [[PubMed](#)]

3. Suda, T.; Yokoo, T.; Kanefuji, T.; Kamimura, K.; Zhang, G.; Liu, D. Hydrodynamic Delivery: Characteristics, Applications, and Technological Advances. *Pharmaceutics* **2023**, *15*, 1111. [[CrossRef](#)] [[PubMed](#)]
4. Kumbhari, V.; Li, L.; Piontek, K.; Ishida, M.; Fu, R.; Khalil, B.; Garrett, C.M.; Liapi, E.; Kalloo, A.N.; Selaru, F.M. Successful liver-directed gene delivery by ERCP-guided hydrodynamic injection (with videos). *Gastrointest. Endosc.* **2018**, *88*, 755–763.e5. [[CrossRef](#)]
5. Hickman, M.A.; Malone, R.W.; Lehmann-Bruinsma, K.; Sih, T.R.; Knoell, D.; Szoka, F.C.; Walzem, R.L.; Carlson, D.M.; Powell, J.S.; Shekhar, S.; et al. Gene expression following direct injection of DNA into liver. *Hum. Gene Ther.* **1994**, *5*, 1477–1483. [[CrossRef](#)] [[PubMed](#)]
6. Budker, V.; Zhang, G.; Knechtle, S.; A Wolff, J. Naked DNA delivered intraportally expresses efficiently in hepatocytes. *Gene Ther.* **1996**, *3*, 593–598. [[PubMed](#)]
7. Liu, F.; Song, Y.K.; Liu, D. Hydrodynamics-based transfection in animals by systemic administration of plasmid DNA. *Gene Ther.* **1999**, *6*, 1258–1266. [[CrossRef](#)] [[PubMed](#)]
8. Budker, V.; Wolff, J.A.; Lee, H.-O.; Gallego-Villar, L.; Grisch-Chan, H.M.; Häberle, J.; Thöny, B.; Kruger, W.D.; Hyland, K.A.; Aronovich, E.L.; et al. High Levels of Foreign Gene Expression in Hepatocytes after Tail Vein Injections of Naked Plasmid DNA. *Hum. Gene Ther.* **1999**, *10*, 1735–1737. [[CrossRef](#)]
9. Aliño, S.F.; Crespo, A.; Dasí, F. Long-term therapeutic levels of human alpha-1 antitrypsin in plasma after hydrodynamic injection of nonviral DNA. *Gene Ther.* **2003**, *10*, 1672–1679. [[CrossRef](#)]
10. Yoshino, H.; Hashizume, K.; Kobayashi, E. Naked plasmid DNA transfer to the porcine liver using rapid injection with large volume. *Gene Ther.* **2006**, *13*, 1696–1702. [[CrossRef](#)]
11. Aliño, S.F.; Herrero, M.J.; Noguera, I.; Dasí, F.; Sánchez, M. Pig liver gene therapy by noninvasive interventionist catheterism. *Gene Ther.* **2007**, *14*, 334–343. [[CrossRef](#)] [[PubMed](#)]
12. Suda, T.; Suda, K.; Liu, D. Computer-assisted Hydrodynamic Gene Delivery. *Mol. Ther.* **2008**, *16*, 1098–1104. [[CrossRef](#)] [[PubMed](#)]
13. Fabre, J.W.; Whitehorne, M.; Grehan, A.; Sawyer, G.J.; Zhang, X.; Davenport, M.; Rela, M.; Eastman, S.J.; Baskin, K.M.; Hodges, B.L.; et al. Critical Physiological and Surgical Considerations for Hydrodynamic Pressurization of Individual Segments of the Pig Liver. *Hum. Gene Ther.* **2011**, *22*, 879–887. [[CrossRef](#)] [[PubMed](#)]
14. Sendra, L.; Herrero, M.J.; Aliño, S.F. Translational Advances of Hydrofection by Hydrodynamic Injection. *Genes* **2018**, *9*, 136. [[CrossRef](#)] [[PubMed](#)]
15. Sendra, L.; Miguel, A.; Pérez-Enguix, D.; Herrero, M.J.; Montalvá, E.; García-Gimeno, M.A.; Noguera, I.; Díaz, A.; Pérez, J.; Sanz, P.; et al. Studying Closed Hydrodynamic Models of “In Vivo” DNA Perfusion in Pig Liver for Gene Therapy Translation to Humans. *PLoS ONE* **2016**, *11*, e0163898. [[CrossRef](#)] [[PubMed](#)]
16. Carreño, O.; Sendra, L.; Montalvá, E.; Miguel, A.; Orbis, F.; Herrero, M.; Noguera, I.; Aliño, S.; Lopez-Andujar, R. A Surgical Model for Isolating the Pig Liver in vivo for Gene Therapy. *Eur. Surg. Res.* **2013**, *51*, 47–57. [[CrossRef](#)] [[PubMed](#)]
17. Sendra, L.; Herrero, M.J.; Montalvá, E.M.; Noguera, I.; Orbis, F.; Díaz, A.; Fernández-Delgado, R.; López-Andújar, R.; Aliño, S.F. Efficacy of interleukin 10 gene hydroflection in pig liver vascular isolated ‘in vivo’ by surgical procedure with interest in liver transplantation. *PLoS ONE* **2019**, *14*, e0224568. [[CrossRef](#)]
18. Kamimura, K.; Kanefuji, T.; Suda, T.; Yokoo, T.; Zhang, G.; Aoyagi, Y.; Liu, D. Liver lobe-specific hydrodynamic gene delivery to baboons: A preclinical trial for hemophilia gene therapy. *Mol. Ther. Nucleic Acids* **2023**, *32*, 903–913. [[CrossRef](#)]
19. Gisbert, L.S.; Matas, A.M.; Ortí, L.S.; Herrero, M.J.; Olivas, L.S.; Orón, E.M.M.; Frasson, M.; López, R.A.; López-Andújar, R.; Ximénez, E.G.; et al. Efficacy of hydrodynamic interleukin 10 gene transfer in human liver segments with interest in transplantation. *Liver Transplant.* **2017**, *23*, 50–62. [[CrossRef](#)]
20. Gao, Q.; DeLaura, I.F.; Anwar, I.J.; Kesseli, S.J.; Kahan, R.; Abraham, N.; Asokan, A.; Barbas, A.S.; Hartwig, M.G. Gene Therapy: Will the Promise of Optimizing Lung Allografts Become Reality? *Front. Immunol.* **2022**, *13*, 931524. [[CrossRef](#)]
21. Hirschfield, G.M.; Gibbs, P.; Griffiths, W.J.H. Adult liver transplantation: What non-specialists need to know. *BMJ* **2009**, *338*, b1670. [[CrossRef](#)]
22. Rodriguez-Perálvarez, M.; Rico-Juri, J.M.; Tsochatzis, E.; Burra, P.; De la Mata, M.; Lerut, J. Biopsy-proven acute cellular rejection as an efficacy endpoint of randomized trials in liver transplantation: A systematic review and critical appraisal. *Transpl. Int.* **2016**, *29*, 961–973. [[CrossRef](#)] [[PubMed](#)]
23. Carlini, V.; Noonan, D.M.; Abdalalem, E.; Goletti, D.; Sansone, C.; Calabrone, L.; Albini, A. The multifaceted nature of IL-10: Regulation, role in immunological homeostasis and its relevance to cancer, COVID-19 and post-COVID conditions. *Front. Immunol.* **2023**, *14*, 1161067. [[CrossRef](#)] [[PubMed](#)]
24. Mendiola Pla, M.; Chiang, Y.; Roan, J.N.; Bowles, D.E. *Gene Therapy for Cardiac Transplantation [Internet]*. Heart Transplantation—New Insights in Therapeutic Strategies; IntechOpen Limited: London, UK, 2022. [[CrossRef](#)]
25. Blancho, G.; Gianello, P.; Germana, S.; Baetscher, M.; Sachs, D.H.; LeGuern, C. Molecular identification of porcine interleukin 10: Regulation of expression in a kidney allograft model. *Proc. Natl. Acad. Sci. USA* **1995**, *92*, 2800–2804. [[CrossRef](#)]
26. Liu, K.S.; Fan, X.Q.; Zhang, L.; NA Wen, Q.; Feng, J.H.; Chen, F.C.; Luo, J.M.; Sun, W.B. Effects of recombinant human interleukin-10 on Treg cells, IL-10 and TGF- β in transplantation of rabbit skin. *Mol. Med. Rep.* **2013**, *9*, 639–644. [[CrossRef](#)]
27. Martins, S.; de Perrot, M.; Imai, Y.; Yamane, M.; Quadri, S.; Segall, L.; Dutly, A.; Sakiyama, S.; Chaparro, A.; Davidson, B.; et al. Transbronchial administration of adenoviral-mediated interleukin-10 gene to the donor improves function in a pig lung transplant model. *Gene Ther.* **2004**, *11*, 1786–1796. [[CrossRef](#)]

28. Hartog, G.D.; Savelkoul, H.F.J.; Schoemaker, R.; Tijhaar, E.; Westphal, A.H.; de Ruiter, T.; van de Weg-Schrijver, E.; van Neerven, R.J.J. Modulation of Human Immune Responses by Bovine Interleukin-10. *PLoS ONE* **2011**, *6*, e18188. [[CrossRef](#)]
29. Kondo, T.; Kobayashi, J.; Saitoh, T.; Maruyama, K.; Ishii, K.J.; Barber, G.N.; Komatsu, K.; Akira, S.; Kawai, T. DNA damage sensor MRE11 recognizes cytosolic double-stranded DNA and induces type I interferon by regulating STING trafficking. *Proc. Natl. Acad. Sci. USA* **2013**, *110*, 2969–2974. [[CrossRef](#)]
30. Katashiba, Y.; Miyamoto, R.; Hyo, A.; Shimamoto, K.; Murakami, N.; Ogata, M.; Amakawa, R.; Inaba, M.; Nomura, S.; Fukuhara, S.; et al. Interferon- α and interleukin-12 are induced, respectively, by double-stranded DNA and single-stranded RNA in human myeloid dendritic cells. *Immunology* **2011**, *132*, 165–173. [[CrossRef](#)]
31. Seldon, P.M.; Barnes, P.J.; Giembycz, M.A. Interleukin-10 does not mediate the inhibitory effect of PDE-4 inhibitors and other cAMP-elevating drugs on lipopolysaccharide-induced tumor necrosis factor- α generation from human peripheral blood monocytes. *Cell Biochem. Biophys.* **1998**, *29*, 179–201. [[CrossRef](#)] [[PubMed](#)]
32. Assadias, S.; Mooney, N.; Nicknam, M.H. Cytokines in Liver Transplantation. *Cytokine* **2021**, *148*, 155705. [[CrossRef](#)]
33. Saxton, R.A.; Tsutsumi, N.; Su, L.L.; Abhiraman, G.C.; Mohan, K.; Henneberg, L.T.; Aduri, N.G.; Gati, C.; Garcia, K.C. Structure-based decoupling of the pro- and anti-inflammatory functions of interleukin-10. *Science* **2021**, *371*, 1222. [[CrossRef](#)]
34. Nagata, K.; Nishiyama, C. IL-10 in Mast Cell-Mediated Immune Responses: Anti-Inflammatory and Proinflammatory Roles. *Int. J. Mol. Sci.* **2021**, *22*, 4972. [[CrossRef](#)]
35. Lu, L.; Barbi, J.; Pan, F. The regulation of immune tolerance by FOXP3. *Nat. Rev. Immunol.* **2017**, *17*, 703–717. [[CrossRef](#)]
36. Whitehouse, G.; Gray, E.; Mastoridis, S.; Merritt, E.; Kodela, E.; Yang, J.H.M.; Danger, R.; Mairal, M.; Christakoudi, S.; Lozano, J.J.; et al. IL-2 therapy restores regulatory T-cell dysfunction induced by calcineurin inhibitors. *Proc. Natl. Acad. Sci. USA* **2017**, *114*, 7083–7088. [[CrossRef](#)]
37. Steen, E.H.; Wang, X.; Balaji, S.; Butte, M.J.; Bollyky, P.L.; Keswani, S.G. The Role of the Anti-Inflammatory Cytokine Interleukin-10 in Tissue Fibrosis. *Adv. Wound Care* **2020**, *9*, 184–198. [[CrossRef](#)]
38. Iyer, S.S.; Cheng, G. Role of Interleukin 10 transcriptional regulation in inflammation and autoimmune disease. *Crit. Rev. Immunol.* **2012**, *32*, 23–63. [[CrossRef](#)] [[PubMed](#)]
39. Oh, S.A.; Liu, M.; Nixon, B.G.; Kang, D.; Toure, A.; Bivona, M.; Li, M.O. Foxp3-independent mechanism by which TGF- β controls peripheral T cell tolerance. *Proc. Natl. Acad. Sci. USA* **2017**, *114*, E7536–E7544. [[CrossRef](#)] [[PubMed](#)]
40. Zorn, E.; Nelson, E.A.; Mohseni, M.; Porcheray, F.; Kim, H.; Litsa, D.; Bellucci, R.; Raderschall, E.; Canning, C.; Soiffer, R.J.; et al. IL-2 regulates FOXP3 expression in human CD4+CD25+ regulatory T cells through a STAT-dependent mechanism and induces the expansion of these cells in vivo. *Blood* **2006**, *108*, 1571–1579. [[CrossRef](#)] [[PubMed](#)]
41. Skartsis, N.; Peng, Y.; Ferreira, L.M.R.; Nguyen, V.; Ronin, E.; Muller, Y.D.; Vincenti, F.; Tang, Q. IL-6 and TNF α Drive Extensive Proliferation of Human Tregs Without Compromising Their Lineage Stability or Function. *Front. Immunol.* **2021**, *12*, 783282. [[CrossRef](#)]
42. Bagheri, Y.; Babaha, F.; Falak, R.; Yazdani, R.; Azizi, G.; Sadri, M.; Abolhassani, H.; Shekarabi, M.; Aghamohammadi, A. IL-10 induces TGF- β secretion, TGF- β receptor II upregulation, and IgA secretion in B cells. *Eur. Cytokine Netw.* **2019**, *30*, 107–113. [[CrossRef](#)] [[PubMed](#)]
43. Hsu, P.; Santner-Nanan, B.; Hu, M.; Skarratt, K.; Lee, C.H.; Stormon, M.; Wong, M.; Fuller, S.J.; Nanan, R. IL-10 Potentiates Differentiation of Human Induced Regulatory T Cells via STAT3 and Foxo1. *J. Immunol.* **2015**, *195*, 3665–3674. [[CrossRef](#)] [[PubMed](#)]
44. Fondevila, C.; Hessheimer, A.J.; Flores, E.; Vendrell, M.; Muñoz, J.; Escobar, B.; Calatayud, D.; Taurá, P.; Fuster, J.; García-Valdecasas, J.C. Step-by-step guide for a simplified model of porcine orthotopic liver transplant. *J. Surg. Res.* **2011**, *167*, e39–e45. [[CrossRef](#)] [[PubMed](#)]

Disclaimer/Publisher's Note: The statements, opinions and data contained in all publications are solely those of the individual author(s) and contributor(s) and not of MDPI and/or the editor(s). MDPI and/or the editor(s) disclaim responsibility for any injury to people or property resulting from any ideas, methods, instructions or products referred to in the content.